IAEA Research Contract no. 6974/RB

SUMMARY REPORT

'Structural Characterization of Advanced Ceramics Using Neutron Diffractometer Developed by Instituto de Pesquisas Energéticas e Nucleares (IPEN)'

C. B. R. Parente
V. L. Mazzocchi

IPEN-CNEN/SP

I. INTRODUCTION

Neutron diffraction has been frequently used in the characterization of advanced ceramics, e.g. the recently developed high-Tc superconductors. It is well known that neutron diffraction is, in general, used as a supplementary technique for x-ray diffraction giving additional information about a structure primarily refined from x-ray diffraction data. Exceptions are, of course, the determination of magnetic structures and the characterization of a magnetic material.

In structural analysis, single crystals are preferably used instead of powders. Single crystal data gives a more complete and reliable information about the structure than powder data can give. However, to grow a single crystal with a suitable size for neutron diffraction, in particular of a ceramic material, is a formidable, even an unfruitful task. Fortunately, the development of computer programmes that use the profile of a powder pattern for the refinement of structural parameters, rather than the integrated intensities of its peaks, has turned the powder method in a powerful tool for structure determination and for characterization of new materials.

At IPEN, the neutron diffraction group is engaged in a research programme which includes determination of crystalline phases in single- or multiphase systems, development of multiple diffraction as a method for structural analysis and study of the mosaicity of single crystals. To perform researches, the neutron diffraction group utilizes the IPEN neutron diffractometer. To analyse the data taken in the diffractometer, besides the commonly used computer programmes for plotting and editing, the group utilizes the programmes POWLS (Powder Least-Squares programme) and DBWS both for the refinement of structural parameters from x-ray and neutron data, the latter one based on the Rietveld method.

The IPEN neutron diffractometer is a multipurpose instrument installed at the IEA-R1 2 MW research reactor. It is a single detector instrument with a fixed angle for the monochromator. Current wavelength is λ = 1.137 A. Flux at specimen is about 5.10^4 neutrons.cm^{-2}.s^{-1}. Control and data acquisition is provided by an Apple compatible microcomputer. A five-circle goniometer is used for single crystal and texture measurements. This goniometer has an extra axis (Σ) which allows neutron multiple diffraction measurements. The neutron diffraction group is in charge of the diffractometer operation and maintenance.

In the last two years, several researches have been initiated, continued or finished by the neutron diffraction group. A few of them are directly related to the scientific scope of this project, i.e. the study of advanced materials. In what follows, we present the main research lines, developed by the neutron diffraction group in cooperation with other groups. In each line, we included a resume of a research already finished or in progress.

Research line:

DETERMINATION OF CRYSTALLINE PHASES IN SINGLE- OR MULTIPHASE SYSTEMS.

In the determination of crystalline phases, neutron diffraction is applied only on those cases where x-ray diffraction does not lead to reliable results. As an example, we mention a research in progress at our laboratory. It consists in the determination of the ordering structure of a chromium steel. The composition of the steel is Fe_7CrC_x where x assumed a low value, namely 5.6 at %. In such a low concentration, the ordering of the carbon atoms in the structure becomes sligthly more visible when using neutrons instead of x-rays. In this study we are using the programme DBWS for refinement of parameters. The refinement is, presently, being carried out. Another research being developed is related to the determination of high-Tc ceramic conductors. This is a research directly related to the project. It is presented below.

Research: PHASES PRESENT IN HIGH-Tc CERAMIC SUPERCONDUCTORS OF THE Bi-Sr-Ca-Cu-O SYSTEM.

R. Muccillo, E.N.S. Muccillo, V.L. Mazzocchi and C.B.R. Parente
Instituto de Pesquisas Energéticas e Nucleares - IPEN-CNEN/SP

Aiming the characterization of phases, the neutron diffraction group has measured several samples of high-Tc ceramic superconductors of the Bi-Sr-Ca-Cu-O system [1,2]. The samples were synthesized in the Materials Science Division at IPEN. Three superconducting crystalline phases are known to coexist in samples of this system. The ideal compositions of such phases [3] are $Bi_2Sr_2CuO_6$,called 2201 phase, with Tc ~ 20K, $Bi_2Sr_2CaCu_2O_8$, 2212, Tc ~ 85K, and $Bi_2Sr_2Ca_2Cu_3O_{10}$, 2223, Tc ~ 110K. Many research efforts attempting to enhance the volume fraction of the higher Tc 2223 phase have been described in literature [4]. Some are related to the partial substitution of lead for bismuth, which is reported to increase the fraction of the 2223 phase increasing, at same time, the uniformity in the composition of the superconduting phase.

The first powder pattern measured in the IPEN neutron diffractometer showed broad peaks with very low intensity. As can be seen in Fig. 1, only a few peaks are scarcely bigger than the background level. The FWHM for these peaks is about 1.5 degree, a too large value. Both characteristics indicate a sample formed by very small crystallites. Before engaging in a structural analysis to determine the phases present in the sample, we made a few attempts to increase the crytallite size via heat treatment. It is not worthwhile to give here further details about the heat treatment only that it consisted, essentially, in annealing the samples at approximately 1070 K for several hours. All attempts, however, were unsuccessful since the powder patterns for annealed samples showed peaks even less intense than those on Fig. 1. Cumulative mass percent finer vs. diameter graphs, obtained in a Sedigraph 5.100 v 2.03, showed that the particles in the samples are themselves too small to allow a sufficient increase in the

crystallite size. Fig. 2 shows three of such graphs together. They were taken with samples 100, BiPb 2223 and Bi-90. The first one corresponds to the sample used to obtain the powder pattern of Fig. 1, Bi-90 is one of the annealed samples and BiPb 2223 is a sample obtained by a partial substitution of Pb for Bi. The median diameters (the value of the equivalent spherical diameter for mass finer at 50%) for samples 100, Bi-90 and BiPb 2223 are, respectively, 25, 8 and 10.5 μm. A comparison between these values shows that the slightly better signal-to-background ratio found in the powder pattern of sample 100 is, in principle, corroborated by a median diameter three times greater than that of sample Bi-90. Concerning sample BiPb 2223, the quality of its powder pattern is not better than the powder pattern obtained with sample Bi-90. It should be noted that the median diameters for these samples have close values. Powder pattern for sample BiPb 2223 is shown in Fig. 3. For sample Bi-90, as well as for other annealed sample (107), only a few peaks were measured for comparison with the corresponding peaks on the pattern for sample 100. The research proceeds with new attempts to obtain samples having larger crystallites.

REFERENCES

[1] CHU, C.W. et al. Phys. Rev. Lett. 60, 941, 1988.
[2] HAZEN, R.M. et al. Phys. Rev. Lett. 60, 1174, 1988
[3] XU, Z. et al. J. Mater. Res., 5, 1, 39, 1990.
[4] YAN, L.C.; STEVENS, R. J. Amer. Ceram. Soc. 75, 1142, 1150 and 1160, 1992.

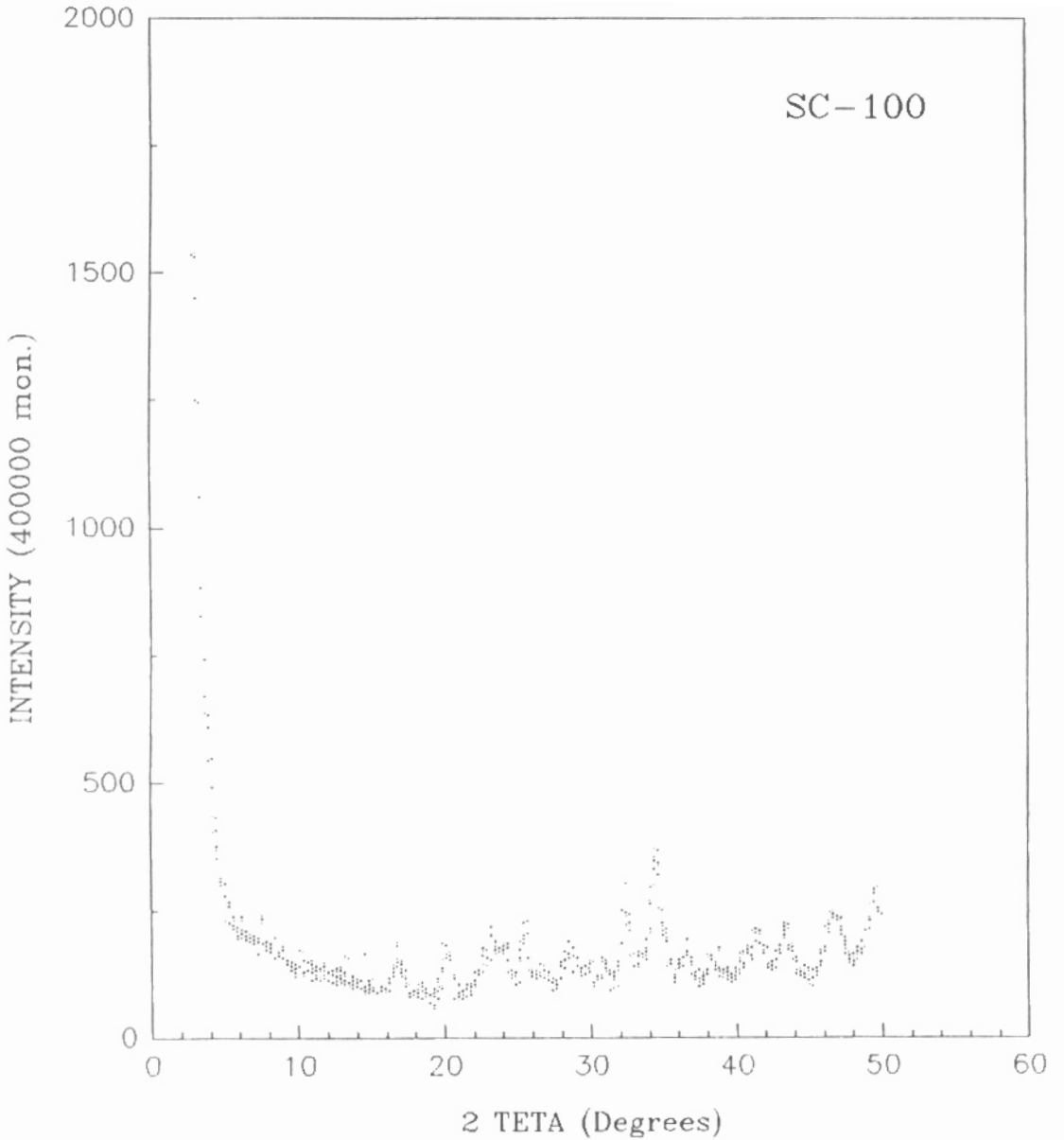

Figure 1 - Neutron powder pattern for a ceramic superconductor of the Bi-Sr-Ca-Cu-O system (sample 100). Owing to the effect of multiple scattering, peaks are not sharp as in a normal pattern.

Superconductor

SediGraph 5100 V2.03 PAGE 1

SAMPLE DIRECTORY/NUMBER: DATA1 /183
SAMPLE ID: Bi 90
SUBMITTER: REGINALDO
OPERATOR: YONE
SAMPLE TYPE: Bi 90
LIQUID TYPE: Water
ANALYSIS TEMP: 35.8 deg C RUN TYPE: High Speed

UNIT NUMBER: 1
START 00:00:00 00/00/00
REPRT 00:00:00 00/00/00
TOT RUN TIME 0:12:02
SAM DENS: 5.6300 g/cc
LIQ DENS: 0.9938 g/cc
LIQ VISC: 0.7118 cp

CUMULATIVE MASS PERCENT FINER VS. DIAMETER
\+ 183 Bi 90
* 184 Bi Pb 2223
o 187 100

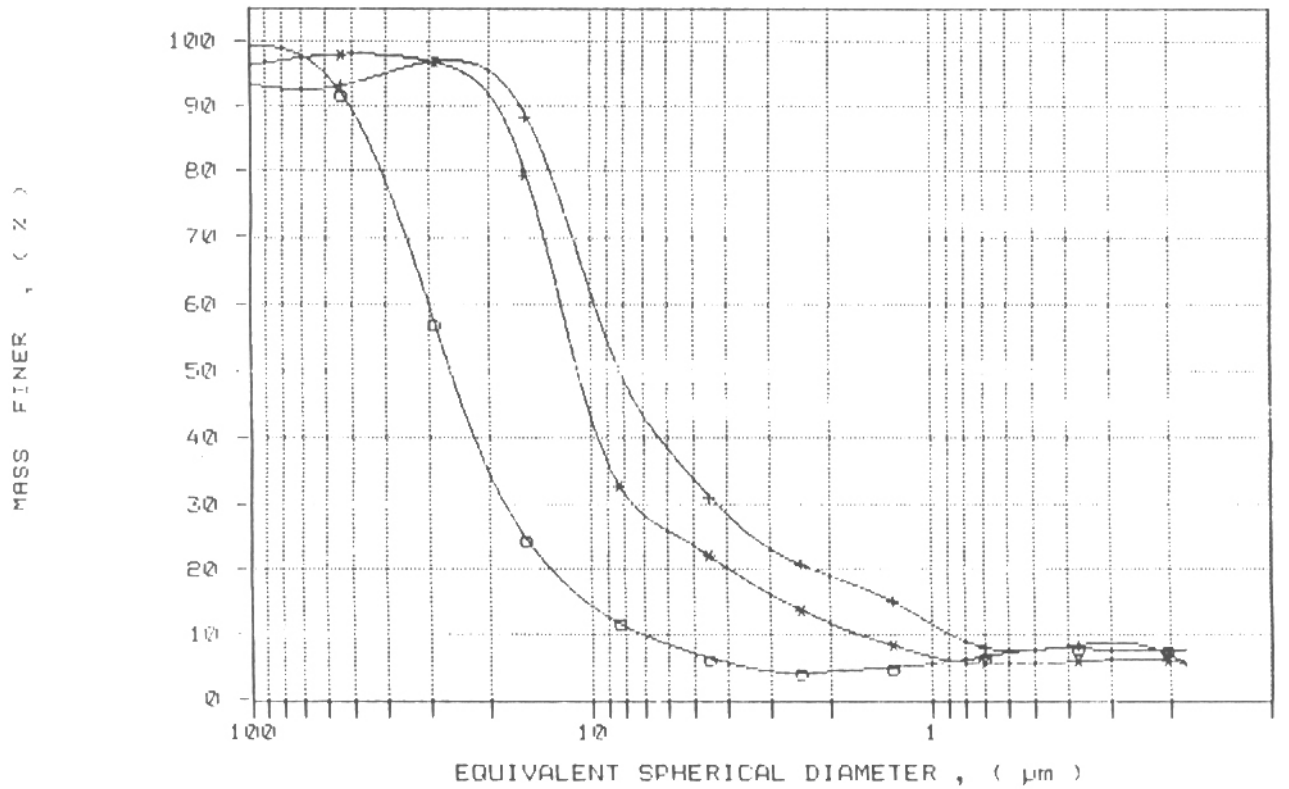

Figure 2 - Particle size distribution for three different superconductor samples.

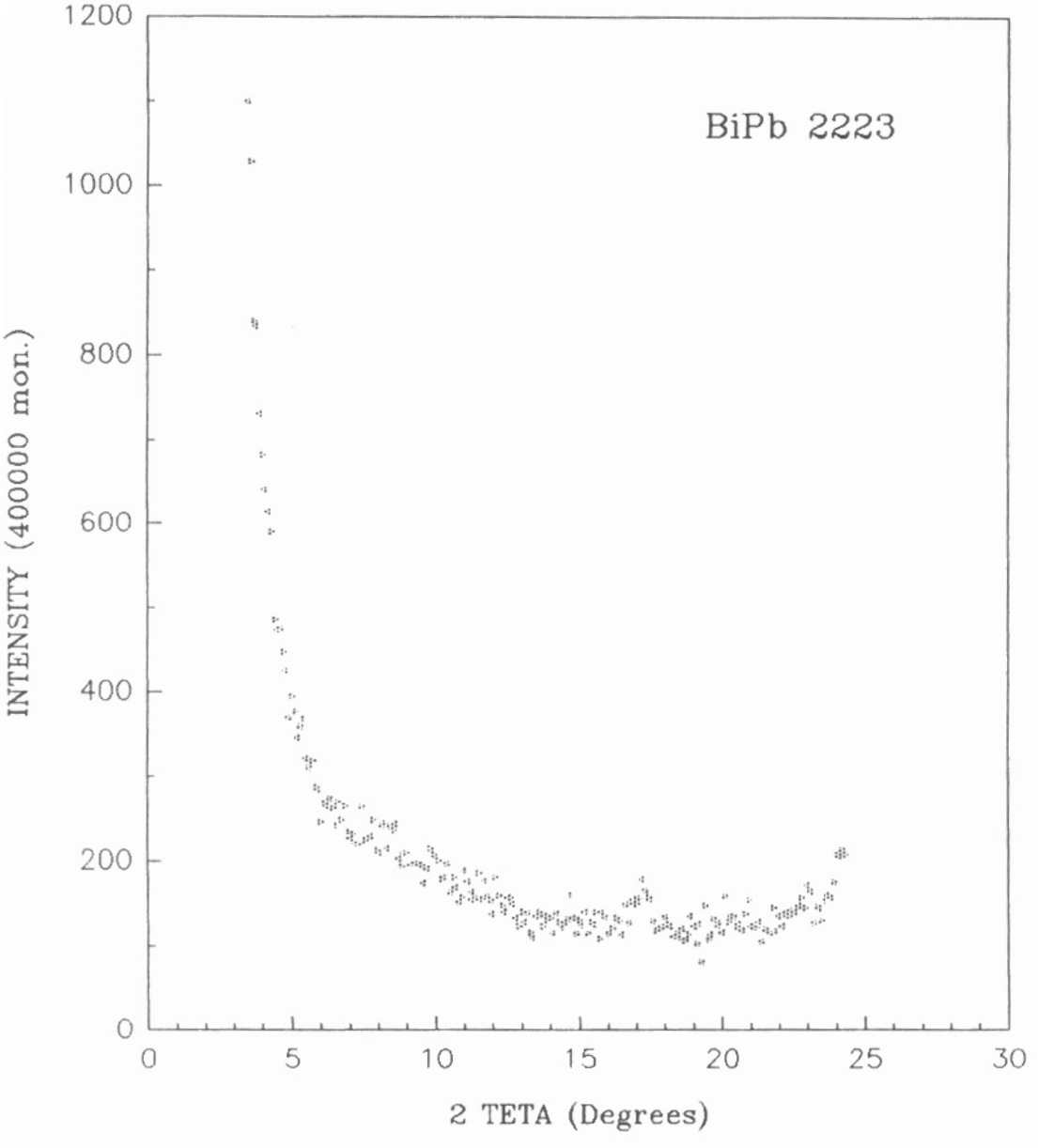

Figure 3 - Neutron powder pattern for a ceramic superconductor of the (Bi,Pb)-Sr-Ca-Cu-O system (sample BiPb 2223). The effect of multiple scattering is remarkable in this pattern.

Research line:

DEVELOPMENT OF X-RAY AND NEUTRON MULTIPLE DIFFRACTION AS A METHOD FOR STRUCTURAL ANALYSIS

In 1984, Mazzocchi studied the α and β phases of quartz by using neutron multiple diffraction (n.m.d.) as a method for structural analysis [1]. As far as we know, this was the first time the general phenomenon of diffraction was used in structural analysis. The analyses of both phases of quartz were performed by using a computer programme, MULTI [2],written to simulate n.m.d. patterns. MULTI uses approximate intensity solutions derived for a many-beam case [3]. These solutions are based in the nowadays called iterative method [4] for the calculation of intensities. This method is an extension to high absorption and high secondary extinction cases of the theory developed by Moon & Shull for the multiple diffraction of neutrons in a mosaic crystal [5]. Moon & Shull calculated the intensity of a particular beam by summing the terms of a Taylor series expansion of the powers of the different beams participating in the phenomenon. They presented analytical formulae retaining terms up to the third order. A low order limitates the calculation of intensities to cases of low absorption and low secondary extinction. These cases are, in general, possible for thin crystals. Thin crystals plus neutron diffraction, on the other hand, is not a good combination since diffracted intensities are very weak in such a case. In 1974, Parente & Caticha-Ellis derived the general term for the Taylor series expansion [6]. With the general term and a computer, it became possible to calculate intensities in an iterative way till any desired order. Parente & Caticha-Ellis made an application of the general term to the calculation of intensities in the n.m.d. from a thick aluminum single crystal [7]. Owing to the high secondary extinction affecting the intensities, good agreement between experimental and calculated intensities was found only for expansions retaining more than ten terms. An x-ray version of MULTI, MULTX, has been recently applied in the study of epitaxial [8] and heteroepitaxial [9] semiconductor layers. More recently, MULTI has been applied in the refinement of the ferri- and paramagnetic phases of magnetite. A resume of this work is given below.

Research: REFINEMENT OF THE FERRI- AND PARAMAGNETIC PHASES OF MAGNETITE MEASURED BY NEUTRON MULTIPLE DIFFRACTION

V.L. Mazzocchi and C.B.R. Parente
Instituto de Pesquisas Energéticas e Nucleares - IPEN-CNEN/SP

According to Verwey and co-workers [10,11,12,13], magnetite (Fe_3O_4) is an inverted Fe spinel of the type $Fe^{3+}(Fe^{2+}Fe^{3+})O_4^{2-}$. The inverted spinel structure of magnetite has a large unit cell containing 8 Fe^{3+} ions in tetrahedral A sites and 8Fe^{2+}plus remaining 8 Fe^{3+} ions in octahedral B sites. Ions in magnetite are distributed in the following positions of space group Fd3m the origin being taken at center ($\bar{4}$3m), -1/8, -1/8, -1/8 from center ($\bar{3}$m): O^{2-} in 32(e), Fe^{2+} and Fe^{3+}, in equal number and at random, in 16(d) and Fe^{3+} in 8(a).

In an ideal spinel structure x is equal to 3/8 (0.375), the arrangement of the O^{2-} ions equaling exactly a cubic close packing. In the inverted spinel structure of magnetite, as well as in many other spinel-like structures, x slightly exceeds 3/8 causing a distortion in the close packing of the O^{2-} ions [12].

The magnetic structure of magnetite, at room temperature, is type Néel A-B [14], i.e. the ions on the A,B sites are coupled antiferromagnetically. In such a coupling, the contribution of the ferric ions is

null since they are distributed in equal numbers on both A and B sites. On the other hand, the contribution of the ferrous ions is maximum since all of them are on the B sites. This ferrimagnetic structure of magnetite has been confirmed by Shull, Wollan and Koehler [15] using neutron powder diffraction data in the analysis. Above ca. 580°C, magnetite is magnetically disordered, i.e. it is a paramagnet.

The measurements of the n.m.d. patterns of both phases were carried out with a natural crystal of magnetite of unknown purity. To heat the crystal, an appropriate cylindrical resistance furnace was employed. This furnace is the same used by the authors in a study of β-quartz using n.m.d. as a method of analysis [2]. A goniometer head linked the furnace to the ϕ-axis allowing for a previous orientation of the crystal in the neutron beam. Room temperature measurements were made with the crystal inside the furnace.

The measurements were carried out after a careful orientation of the 111 reflection. Since this reflection is almost entirely due to magnetic scattering and very strong [15] the n.m.d. pattern obtained at room temperature is type 'Aufhellung'. For the high temperature measurements, the temperature was stabilized at 703°C, well above the transition. At this temperature, owing to the random orientation of the magnetic moments, 111 reflection is reduced to the nuclear contribution and, consequently, is very weak. For this reason, the n.m.d. pattern is a combination 'Aufhellung-Umweganregung'. The ϕ-scans for both patterns were carried out in steps of 0.1^{o}, 5 min of counting time each step, over an azimuthal angular interval extending from 0 to 83.5^{o}.

In the refinement of the structural parameters a process based on the parameter-shift method [16] was employed. The reliability factor used in the refinements is given by

$$R = \frac{\sum_{k} |I_k(obs) - I_k(calc)|}{\sum_{k} I_k(obs)}$$

where $I_k(obs)$ and $I_k(calc)$ are respectively the observed and the calculated intensities; c is a scale factor which is varied in order to minimize R, for each value assumed for the parameter in its interval of variation. The refinements were made in a point-to-point basis, i.e., for each experimental value $I_k(obs)$ a corresponding theoretical value $I_k(calc)$ was calculated by MULTI using a given set of structural parameters. In a first refinement (I) a same isotropic thermal parameter B was assumed for all ions in the structure. In a second refinement (II) different parameters were assumed for the special positions in the space group. They are identified in this case by B_a, B_d and B_e for the positions 8(a), 12(d) and 32(e), respectively. Finally, in a third refinement (III), anisotropic thermal parameters were assumed in the calculations.

Fig. 1 shows the experimental n.m.d. pattern obtained for the ferrimagnetic phase in comparison with simulated patterns (full line) obtained after completion of refinements I, II and III (comparisons A., B. and C., respectively). A qualitative evaluation of the three comparisons shows that C. far exhibits the best agreement between experimental and simulated patterns, when compared to A. and B. Moreover, A. and B. are almost indistinguishable concerning this aspect. Table I lists the results of refinements I, II and III, for the ferrimagnetic phase. The values of R found for the three refinements confirm the above assertions. At this point it is important to note that in refinement III mosaic spread η was refined together with the structural parameters. In refinements I and II it was considered constant and equal 0.0044 rad, a value obtained from a rocking curve of the 111 ferrimagnetic reflection.

Fig. 2 is the equivalent of Fig. 1 for the paramagnetic phase. Nevertheless, differently from Fig. 1, an evaluation of the refinements I, II and III (comparisons A,. B. and C., respectively) shows no remarkable differences between A., B. and C. In fact, the values of R in Table I, which also lists the results of refinements I, II and III for the paramagnetic phase, are very close although diminishing from refinement I thru III. Here, like in the ferrimagnetic case, η was maintained constant in the first two refinements with the value 0.0044 rad, obtained from a rocking curve of the 111 paramagnetic reflection.

To verify the consistency of the values for the lattice parameter a found in the refinements I, II and III for the paramagnetic phase, the variation of this parameter with temperature was calculated using the coefficients of linear expansion for magnetite determined by Sharma [17] for temperatures below and above the transition. Fig. 3 shows the curve of variation of a with temperature. The value of a serving as basis in the calculation is that found in the refinement II for the ferrimagnetic phase. It is shown as a square at 30°C. The values obtained in the refinements I and III are also shown in the Figure, as well as those obtained in the refinements I, II and III for the paramagnetic phase. A few other values found in the literature for the ferrimagnetic phase [18] are also shown in the Figure for comparison. They are represented by small full circles.

TABLE I - Lattice, positional and thermal parameters found in the refinements of the ferri- and paramagnetic phases of magnetite.

PHASES		FERRI (30°C)			PARA (703°C)		
SPECIAL POSITIONS	PARAMETERS	REFIN. I	REFIN. II	REFIN. III	REFIN. I	REFIN. II	REFIN. III
	a (A)	8.401(0)	8.402(0)	8.399(6)	8.486(0)	8.490(5)	8.491(3)
	B (A^2)	1.15(0)	-	-	1.42(5)	-	-
8a	B_a (A^2)	-	0.9(0)	-	-	1.8(5)	-
	B_{11} (A^2)	-	-	0.28(0)	-	-	0.26(0)
16d	B_d (A^2)	-	1.1(3)	-	-	1.1(5)	-
	B_{11} (A^2)	-	-	0.63(5)	-	-	0.41(0)
	B_{12} (A^2)	-	-	-0.27(5)	-	-	-0.00(9)
32e	x	0.370(5)	0.370(0)	0.370(7)	0.381(5)	0.381(5)	0.381(7)
	B_e (A^2)	-	1.3(0)	-	-	1.8(0)	-
	B_{11} (A^2)	-	-	0.07(7)	-	-	0.19(8)
	B_{12} (A^2)	-	-	0.00(8)	-	-	0.18(3)
	η (rad)	-	-	0.0062(6)	-	-	0.0051(2)
	C ($x10^5$)	1.620	1.630	2.285	2.040	1.995	2.380
	R (%)	3.99	3.96	3.00	3.56	3.46	3.32

REFERENCES

[1] MAZZOCCHI, V.L. Estudo das fases ferri- e paramagnética da magnetita medidas com difração múltipla de nêutrons. São Paulo, 1992. (Tese de Doutoramento, IPEN-CNEN/SP, Universidade de São Paulo).

[2] MAZZOCCHI, V.L.; PARENTE, C.B.R. Study of β-quartz by neutron multiple diffraction. (To be published in the Journal of Applied Crystallography, 27, 1994)

[3] PARENTE, C.B.R.; MAZZOCCHI, V.L.; PIMENTEL, F.J.F. Approximate intensity solutions for the multiple diffraction of neutrons in a many-beam case. (To be published in the Journal of Applied Crystallography, 27, 1994).
[4] CHANG, S.-L. Multiple diffraction of x-rays in crystals. Springer-Verlag, Berlim-Heidelberg-New York-Tokyo, 1984.
[5] MOON, R.M.; SHULL, C.G. The effects of simultaneous reflections on single-crystal neutron multiple diffraction intensities. Acta Cryst. 17, 805-12, 1964.
[6] PARENTE, C.B.R.; CATICHA-ELLIS, S. Multiple scattering of x-rays and neutrons. I. A recurrence formula for the Taylor series expansion in the calculation of intensities. Japan. J. Appl. Phys. 13, 10, 1501-5. 1974.
[7] PARENTE, C.B.R.; CATICHA-ELLIS, S. Multiple scattering of x-rays and neutrons. II. Neutron multiple scattering by an aluminum single crystal. Japan. J. Appl. Phys. 13, 10, 1506-13. 1974.
[8] SALLES da COSTA, C.A.B.; CARDOSO, L.P.; MAZZOCCHI, V.L.; PARENTE, C.B.R. Multiple diffraction simulation in the study of epitaxial layers. Defect Control in Semiconductors, vol. II, K.Sumino (ed.), pp.1535-1539, Elsevier. Science Publishers B.V. (North-Holland), 1990. Proceedings of The International Conference on the Science and Technology of Defect Control in Semiconductors. Yokohama, Japan, September 17-22, 1989.
[9] SALLES da COSTA, C.A.B.; CARDOSO, L.P.; MAZZOCCHI, V.L.; PARENTE, C.B.R. Simulation of Renninger scans for heteroepitaxic layers. J. Appl. Cryst. , 25, 366-71, 1992.
[10] VERWEY, E.J.W.; de BOER, J.H. Cation arrangement in a few oxides with crystal structures of the spinel type. Rec. Trav. Chim. 55, 531-40, 1936.
[11] VERWEY, E.J.W.; HAAYMAN, P.W. Electronic conductivity and transition point of magnetite (Fe_3O_4). Physica VIII, 9 , 979-87, 1941.
[12] VERWEY, E.J.W.; HEILMANN, E.L. Physical properties and cation arrangement of oxides with spinel structures. I. Cation arrangement in spinels. J. Chem. Phys. 15, 4, 174-80, 1947.
[13] VERWEY, E..J.W.; HAAYMAN, P.W.; ROMEIJN, F.C. Physical properties and cation arrangement of oxides with spinel structures. II. Electronic conductivity. J. Chem. Phys. 15, 4, 181-7, 1947.
[14] NÉEL, L. Propriétés magnétiques des ferrites; ferrimagnétisme et antiferromagnétisme. Ann. Physique. 3, 137-98, 1948.
[15] SHULL, C.G.; WOLLAN, E.O.; KOEHLER, W.C. Neutron scattering and polarization by ferromagnetic materials. Phys. Rev. 84, 5, 912-21, 1951.
[16] BUHIYA, A.K.; STANLEY, E. The refinement of atomic parameters by direct calculation of the minimum residual. Acta Cryst., 16,.981-4 , 1963.
[17] SHARMA, S.S. Thermal expansion of crystals. II. Magnetite and fluorite. Proc. Ind. Acad. Sci. A, 31, 261-75, 1950.
[18] TOMBS, N.C.; ROOKSBY, H.P. Structure transition and antiferromagnetisme in magnetite. Acta Cryst 4, 474-5, 1951
[19] ABRAHAMS, S.C.; CALHOUN, B.A. The low-temperature transition in magnetite. Acta Cryst. 6, 105-6, 1953.
[20] YOSHIDA, J.; IIDA, S. X-ray study of the phase transition in magnetite. J. Phys. Soc. Japan, 47, 5, 1627-33, 1979.

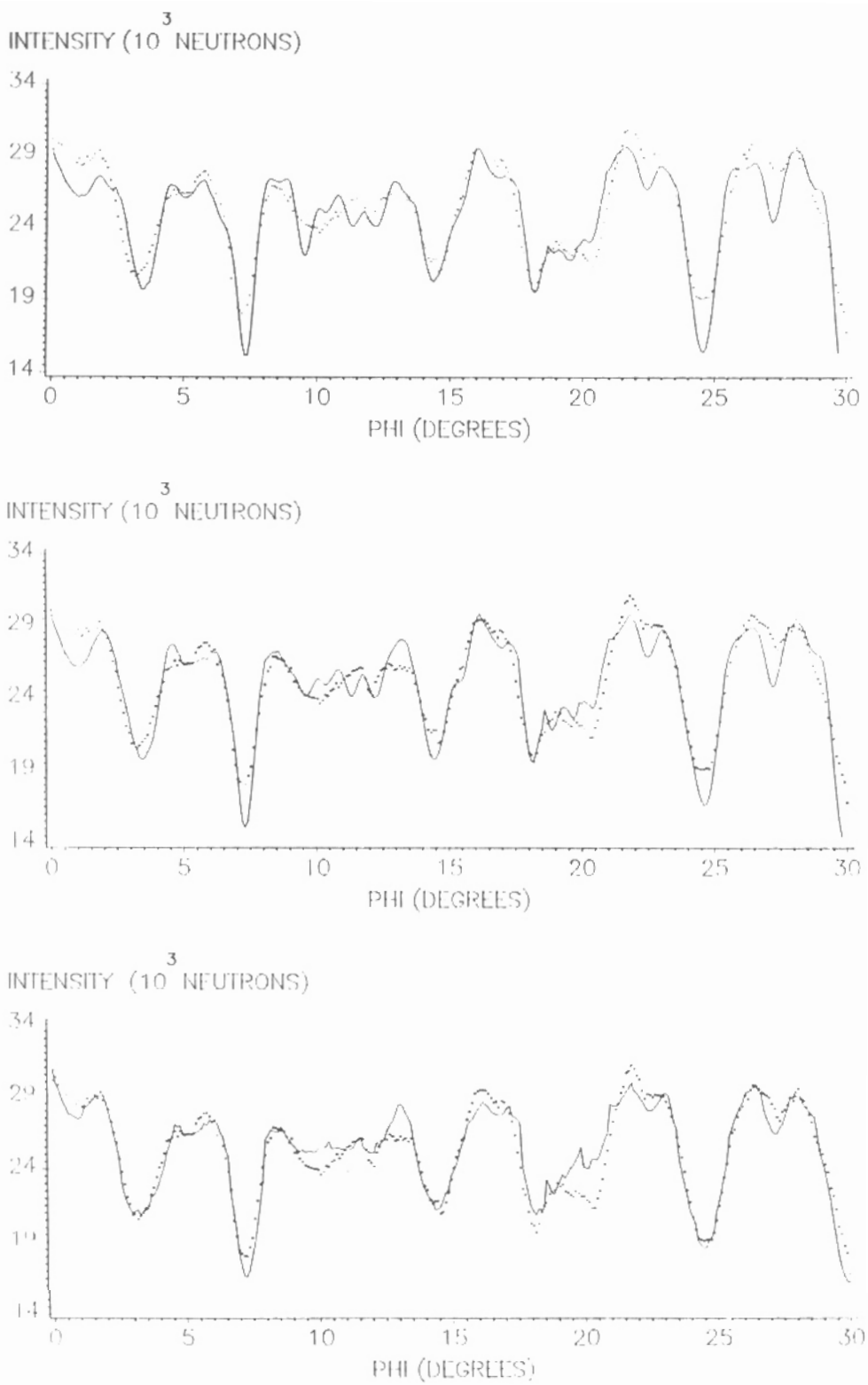

Figure 1 - Comparison between the experimental n.m.d. pattern for the ferrimagnetic phase of magnetite and simulated patterns (full line) after refinements I (A.), II (B.) and III (C.).

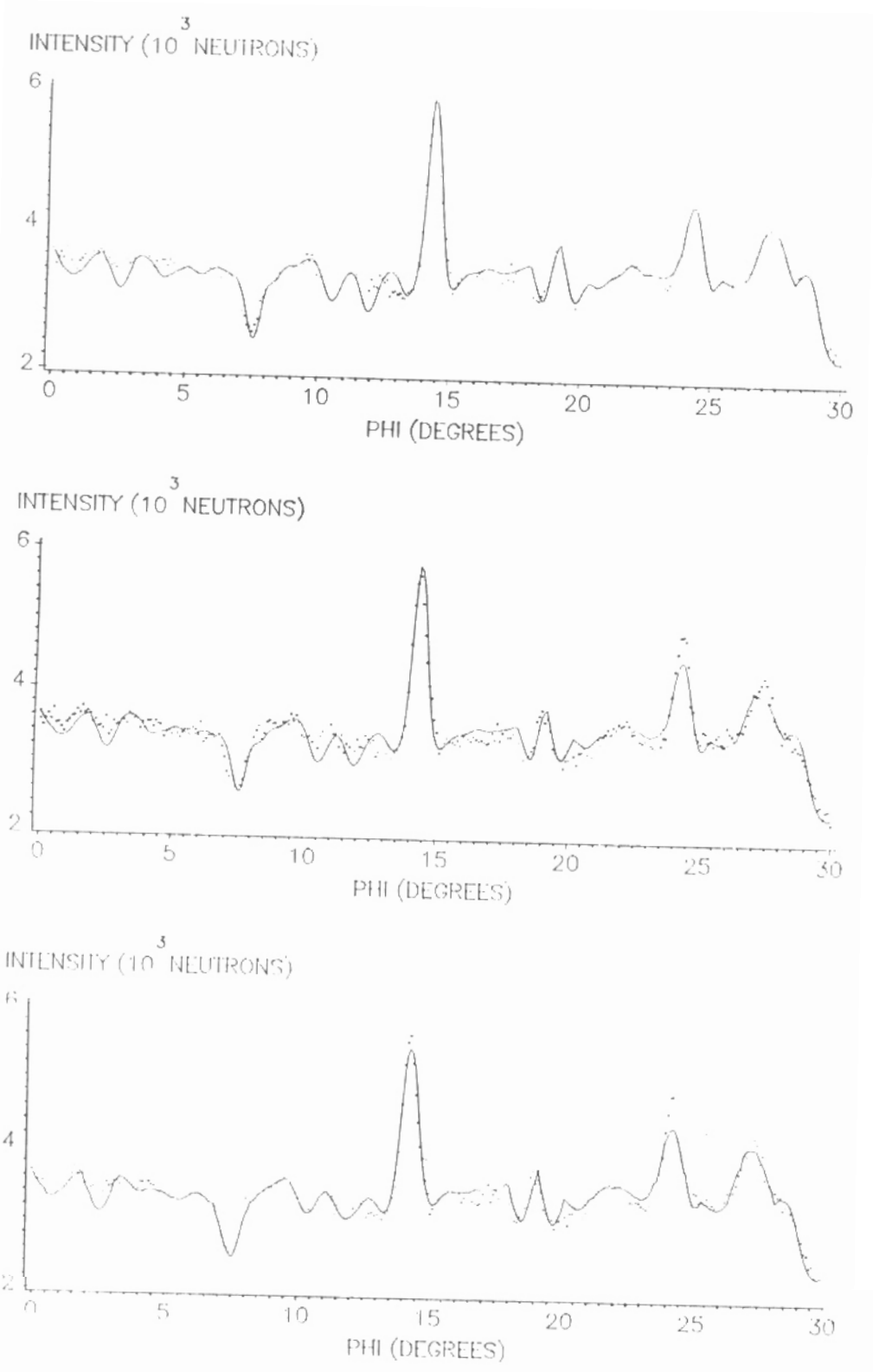

Figure 2 - Comparison between the experimental n.m.d. pattern for the paramagnetic phase of magnetite and simulated patterns (full line) after refinements I (A.), II (B.) and III (C.).

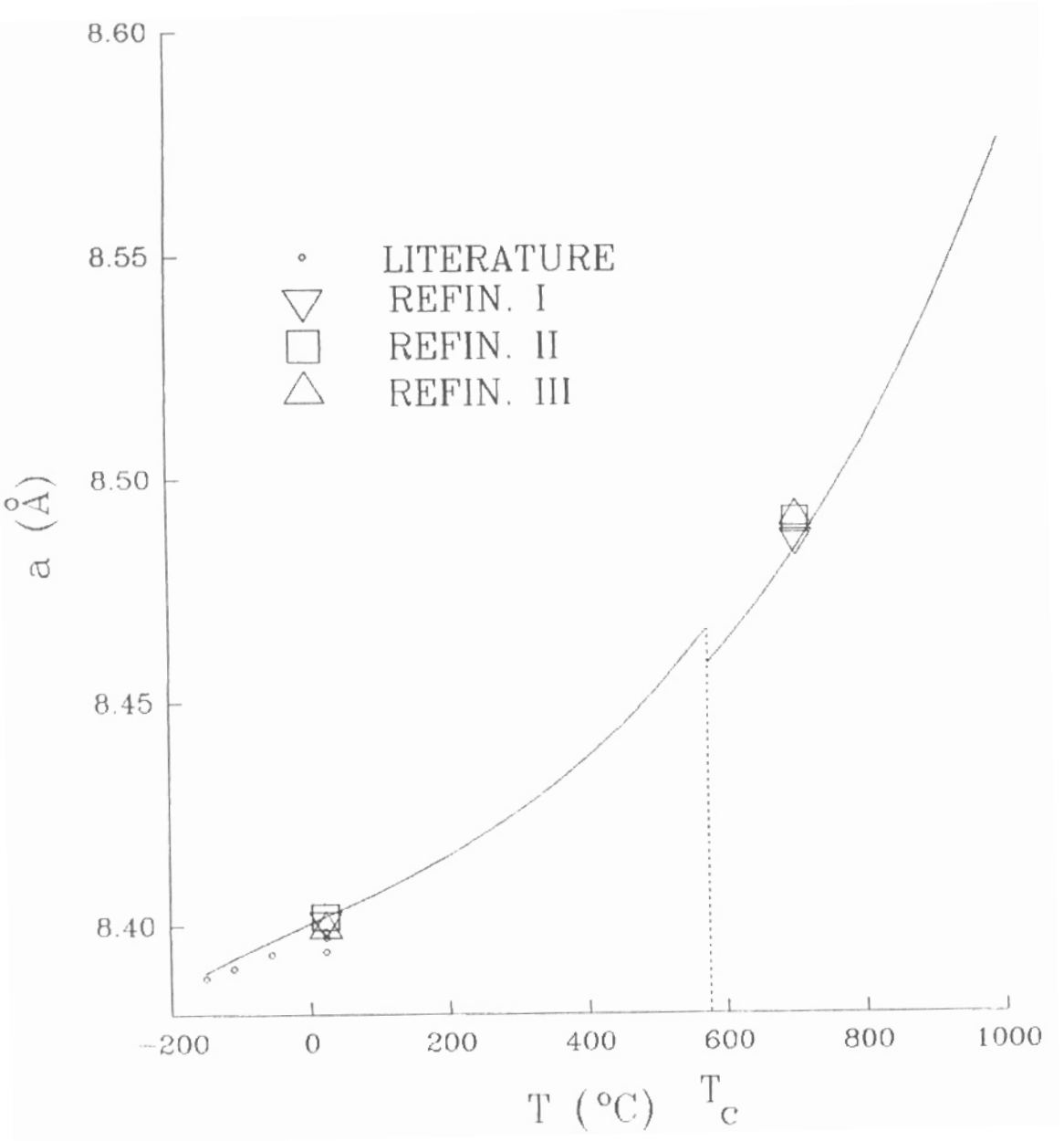

Figure 3 - Curve a vs. T for the verification of the consistency of values found at high temperature.

Research line:

STUDY OF THE MOSAICITY OF SINGLE CRYSTALS

Research: STUDY OF CRYSTALLINE QUALITY OF CZOCHRALSKI GROWN $BaLiF_3$ SINGLE CRYSTALS.

S.L. Baldochi, V.L. Mazzocchi, C.B.R. Parente and S.P. Morato
Instituto de Pesquisas Energéticas e Nucleares - IPEN-CNEN/SP

In this work we study the influence of some characteristics of the growth process in the crystalline quality of Czochralski grown $BaLiF_3$ single crystals. During the growth of a single crystal, it is possible that more than one crystalline domain is formed. In general, the orientations of the domains are very close one to another. The crystalline quality of a crystal, here considered only in its macroscopic aspects, is then dependent on how many domains are formed, the angular width of each one and the angular dispersion between them. This information is, in general, obtained by measuring rocking curves in the moving-crystal-stationary-detector procedure, i.e., the ω-scan in the normal-beam equatorial geometry [1] using x-rays or neutrons. A neutron beam has, in general, a large cross-sectional area and a sample can be completely immersed in the beam. Associated with this characteristic, the high penetration of neutrons in most materials makes possible to observe all domains simultaneously. The same result is not possible with x-rays, for obvious reasons.

Rocking curves measured with neutrons have been used classically to evaluate the quality of monochromators used in neutron diffractometers [2]. In this work, rocking curves are used to establish correlations between the crystalline quality of Czochralski grown $BaLiF_3$ single crystals with three basic aspects of the growth: uniformity of the crystals, growth direction and rotation rate. We measured 8 samples with two different directions of growth, <111> and <100>. Their characteristics are given in Table I together with the reflections observed for each sample. Figure 1 is a representation of a crystal boule with the three considered regions: initial cone, main body and final cone (not used for the measurements). The average diameter of the main body of the samples ranged from 25 to 30 mm and their lengths from 20 to 30 mm. Samples #14C, #15C, #17C and #24I were obtained from experiments where the growth was interrupted by quickly raising the crystal from the melt in order to observe the interface shape. Samples #31 and #38 were obtained from boules after a complete growth. Crystal #38 was cut as showed in Fig. 1. Other crystals were measured in their original shapes.

For each sample we measured at least one rocking curve corresponding to the growth direction. For a few samples we measured four curves by rotating the sample around the growth direction in steps of 90 degrees. This procedure allows the observation of domains that could appear superposed in one of the curves. To observe the crystalline quality in directions other than the growth direction, for samples #24I, #31 and #38 we measured reflections that are perpendicular to the growth direction. For these samples we also measured in the second growth direction considered in the study. For example, measured directions in sample #24I were: <100>, the growth direction, <011>, <01$\bar{1}$>, <0$\bar{1}\bar{1}$>, <0$\bar{1}$1>, which are perpendicular to <100>, and <111> the second direction of growth.

To study the uniformity, we used three samples: #38C, #38 and #31 from two crystals grown in similar conditions: <111> direction, 30 rpm and pulling rate of 1 mm/h. Figures 2 and 3 show, respectively, the measured curves for the 111 reflection at $\phi = 0°$ and 90° and two reflections, 1$\bar{1}$0 and $\bar{1}$10, which are perpendicular to the growth direction.

The cone region shows, in all measurements, more imperfections than the main body region. We observe from the rocking curves measured for samples #38C and #38 that the cone presents two or more

mosaic domains. Due to this fact, it cannot be classified as a mosaic single crystal. This result is empirically known by crystal growers. Cone formation is characterized by changes in the growth rate, as well as in the crystal diameter, and by thermal instability of the melt. Higher thermal instability will obviously result in higher concentration of distortions and defects in the crystalline structure. From the curves we also note that there is a higher dispersion of mosaic domains for the reflections perpendicular to the growth direction, when compared to the dispersion in the growth direction itself. Moreover, when comparing these reflections with the same kind of reflections in the main body, the cone regions continue to present a wider dispersion of mosaic domains. It is noteworthy that for each reflection, although with greater angular dispersion, the results at the cone region agree with the results at the main body region.

The measured curves in the growth direction of the sample #31 (boule) are similar to those obtained with sample #38 (only central region of the crystal). However, the measured curves for the reflections perpendicular to the growth direction show a lower dispersion for sample #38. This implies that sample #38 has a better crystalline quality than sample #31, although they were grown in the same conditions. One of the reasons for this result could be the fact that, when measuring sample #31, both cone and central region contributed to the measured intensity simultaneously. Although the cone contribution is not large compared to the central region, since its volume is several times less the volume of the central region, its presence can impair the observed crystal quality. However, the difference observed between the two samples could be also due to intrinsic characteristics of the crystals. Two crystals obtained in similar conditions will not have exactly the same quality. To verify the influence of the cone in the crystalline quality of sample #31, we measured again this sample with the cone region covered by a cadmium foil. The observed curves showed no appreciable differences from the first ones [3]. For this reason, we conclude that the differences were intrinsic to the crystals and not due to the cone presence. It should be noted that the volume of the cone region is, in general, several times less than the volume of the main body.

We note from Figures 2 and 3 that the angular distance between two mosaic domains in the growth direction was approximately 0.4° and, in the perpendicular directions, 1.5°. So far, it is possible, at least in the growth direction, to consider the studied samples as single crystals.

To study the influence of the growth direction we compared samples #24I and #31 that are crystals grown at, respectively, <100> and <111> directions both with a rotation rate of 30 rpm and a pulling rate of 1 mm/h. Figure 4 shows the measured curve for 100 reflection at $\phi = 0°$ and 90° and for two reflections, 011 and $01\bar{1}$, with scattering vectors perpendicular to the growth direction. It is easy to note that sample #24 is a crystal with a better crystalline quality than sample #31. This is true not only because the rocking curves for the growth direction are very narrow but also because the same are observed in the reflections perpendicular to the growth direction. This is not observed for the samples #38 and #31 both grown in the <111> direction.

Figure 5 shows the rocking curves for samples #24 and #31. A fitting of gaussian curves is also shown in the figure. This fitting allows to determine number and characteristics of the mosaic domains of the crystal. Sample #24 has two mosaic blocks approximately 0.2° apart. One of the domains contributes very little when compared with the other one whose height is approximately three times greater. The half width (β) and the mosaic width (η) of the domains are listed in Table II. Domains are numbered according the increasing values of their angular positions ω. It should be noted that the values for mosaic width in the table are affected by the experimental divergence. Due to the qualitative approach assumed in this work, it was not worthwhile to make the deconvolution of the curves to access the intrinsic values of η. Sample #31 has three mosaic blocks with relative deviations between adjacent domains of approximately 0.5°. The greater domain in this sample has mosaic width of 0.23° which corresponds to approximately twice the mosaic width of sample #24.

To determine the influence of the rotation rate and, consequently, the influence of the interface shape in the quality of the pulled crystals, we measured rocking curves for samples #14C, #15C, 17C and

#38C. These crystals were grown in the <111> direction with the same pulling rate but with rotation rates of 20, 40, 60 and 30 rpm, respectively. These samples are cone regions, where the growth was ended by quickly raising the crystal from the melt to preserve the interface shape, except the #38C. As mentioned before, this sample was cut from a boule according to Fig. 1.

Concerning the rocking curves obtained with samples above (Fig. 6), we noted that: both the convex (#14C) and the concave (#17C) interfaces led to the formation of several mosaic domains. The better quality is observed for the crystals grown with flat (#38C) or semiflat (#15C) interfaces. Similar results are observed for the <100> direction, that is, crystalline quality decreases for convex and concave interfaces of growth.

Table 1 - Characteristics of the samples and measured reflections

CRYSTAL	GROWTH DIRECTION	ROTATION RATE	INTERFACE SHAPE	SAMPLES	MEASURED REFLECTIONS
C#01/89	[100]	10	convex	#01 (main body)	100
I#14/89	[111]	20	semiflat	#14C (cone)	111
I#15/89	[111]	40	flat	#15C (cone)	111
I#17/89	[111]	60	concave	#17C (cone)	111
I#24/90	[100]	30	flat	#24I (boule)	100, 111, 011, $0\bar{1}\bar{1}$, $01\bar{1}$, $0\bar{1}1$
C#31/90	[111]	30	flat	#31 (boule)	111, 100, $0\bar{1}1$, $\bar{1}01$, $1\bar{1}0$, $\bar{1}10$
C#38/90	[111]	30	flat	#38C (cone)	111
				#38 (main body)	111, 100, $02\bar{2}$, $0\bar{2}2$, 202, $\bar{2}02$, $2\bar{2}0$, $\bar{2}20$

Table 2 - Half and mosaic widths of the domains in samples #24 and #31

SAMPLE #24			SAMPLE #31		
domain	β	η	**domain**	β	η
1	0.31	0.13	1	0.54	0.23
2	0.14	0.06	2	0.80	0.34
			3	0.84	0.36

REFERENCES

[1] U. W. Arndt and B. T. M. Willis, Single crystal diffractometry (University Press, Cambridge, 1966).
[2] G. E. Bacon, Neutron diffraction 3a. ed. (Claredon Press, Oxford, 1975).
[3] S. L. Baldochi. Doctor Thesis (University of São Paulo, Brazil, 1993).

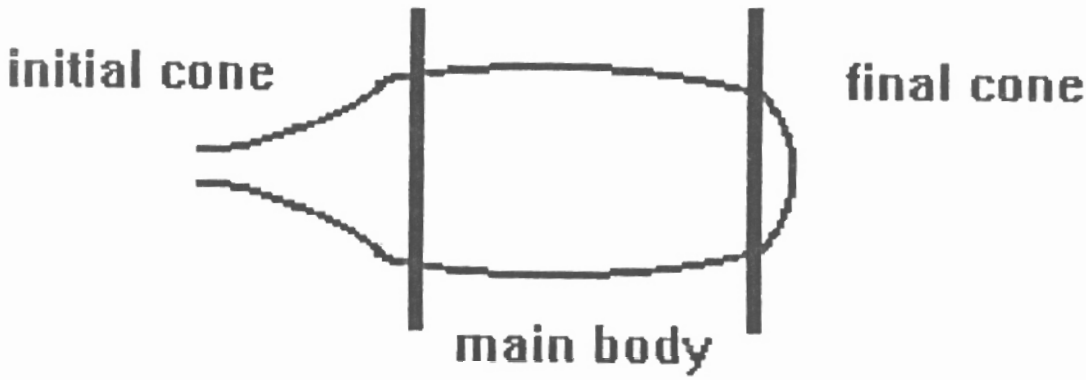

Figure 1 - A representation of a crystal boule with the three regions considered in the measurements.

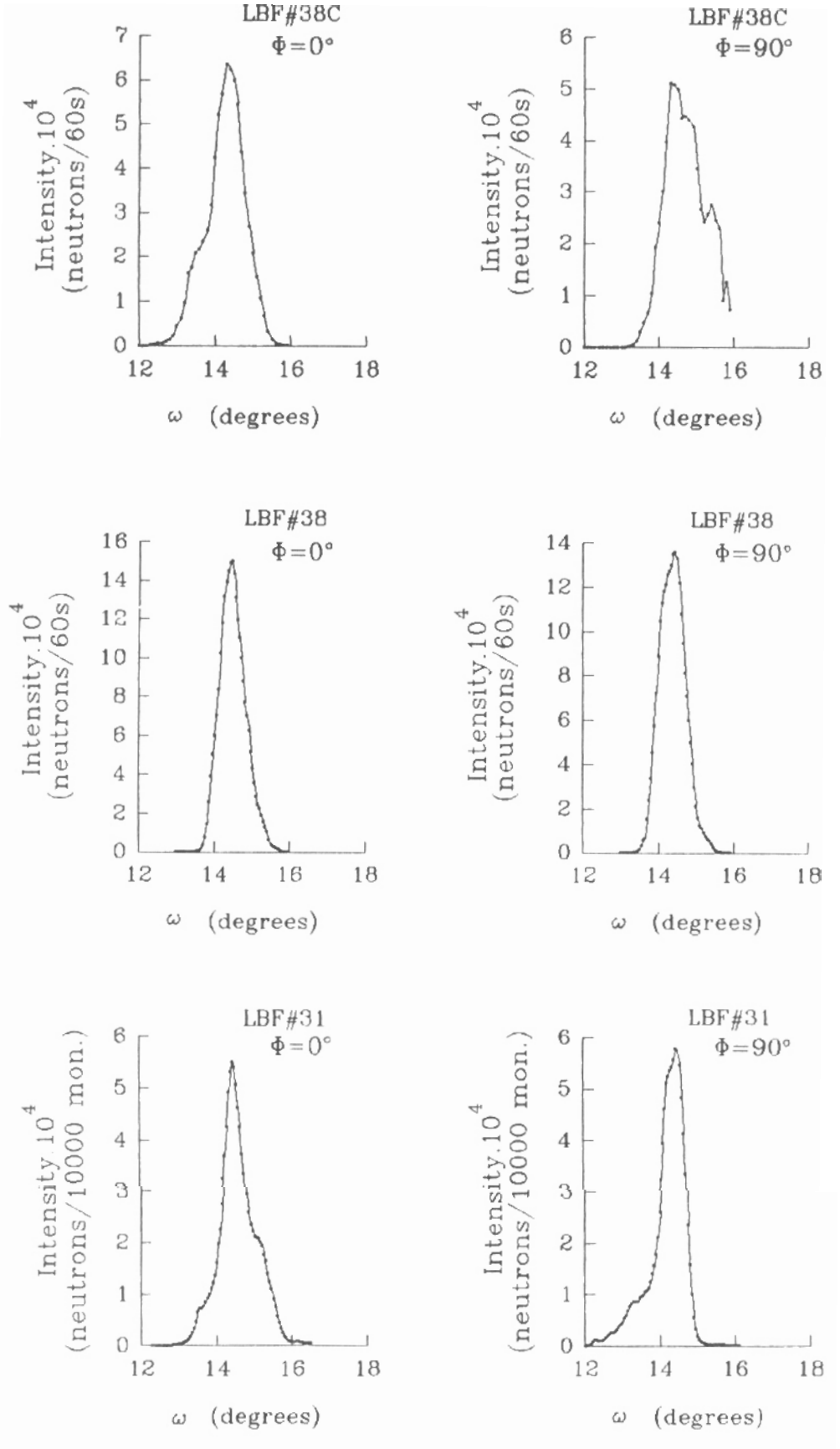

Figure 2 - Rocking curves for the growth direction of samples #38C, #38 and #31.

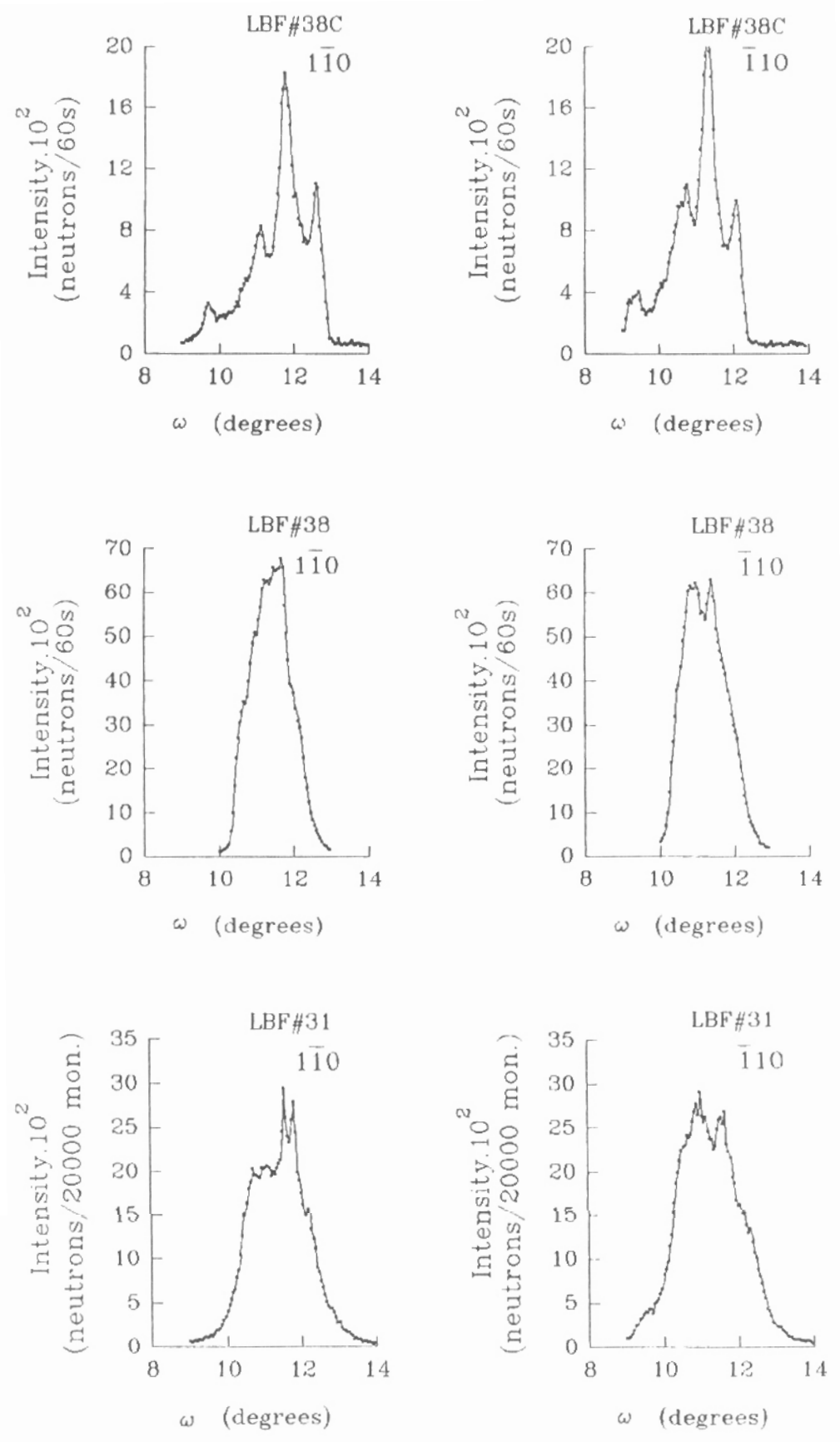

Figure 3 - Rocking curves for reflections perpendicular to the growth direction of samples #38C, #38 and #31.

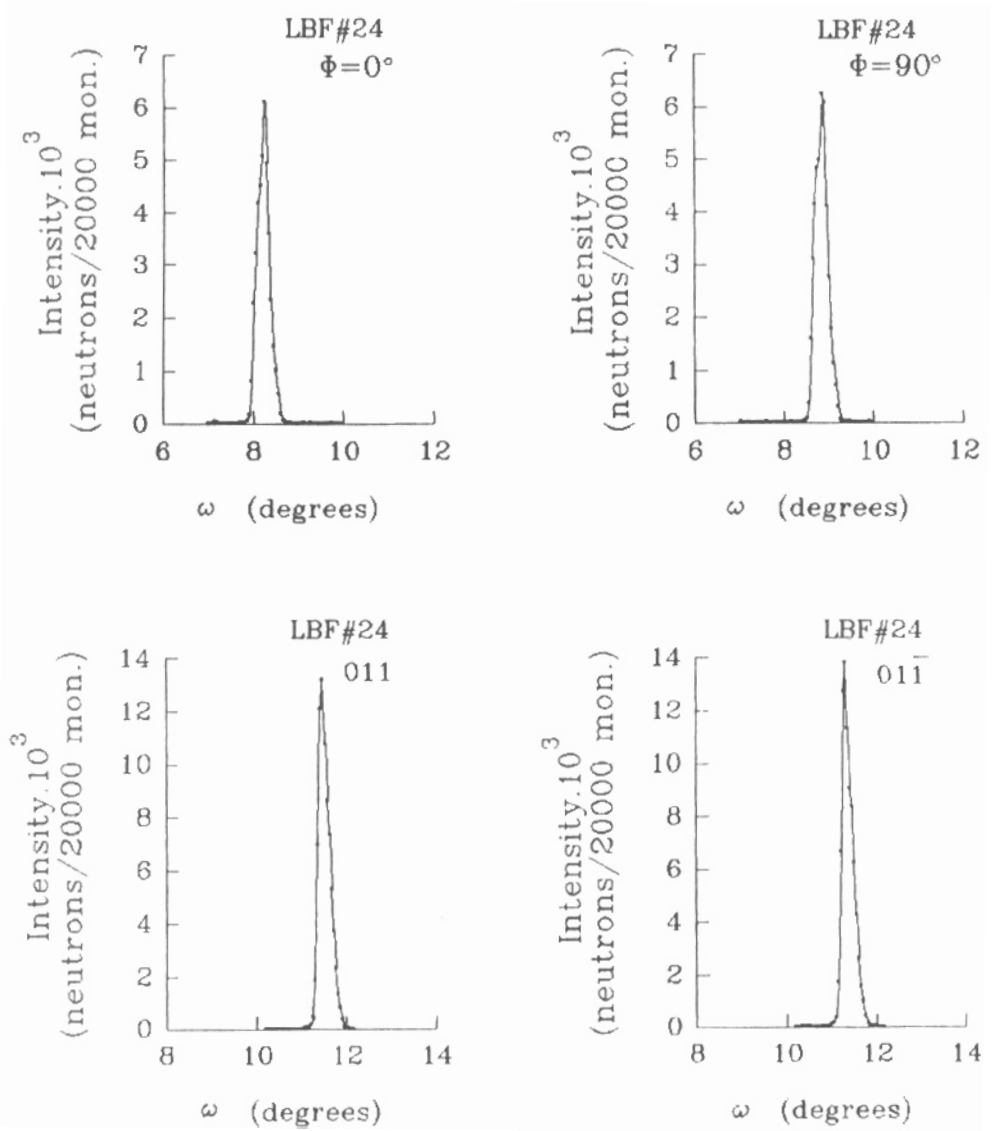

Figure 4 - Rocking curves for the growth direction and for directions perpendicular to the growth direction of sample #24.

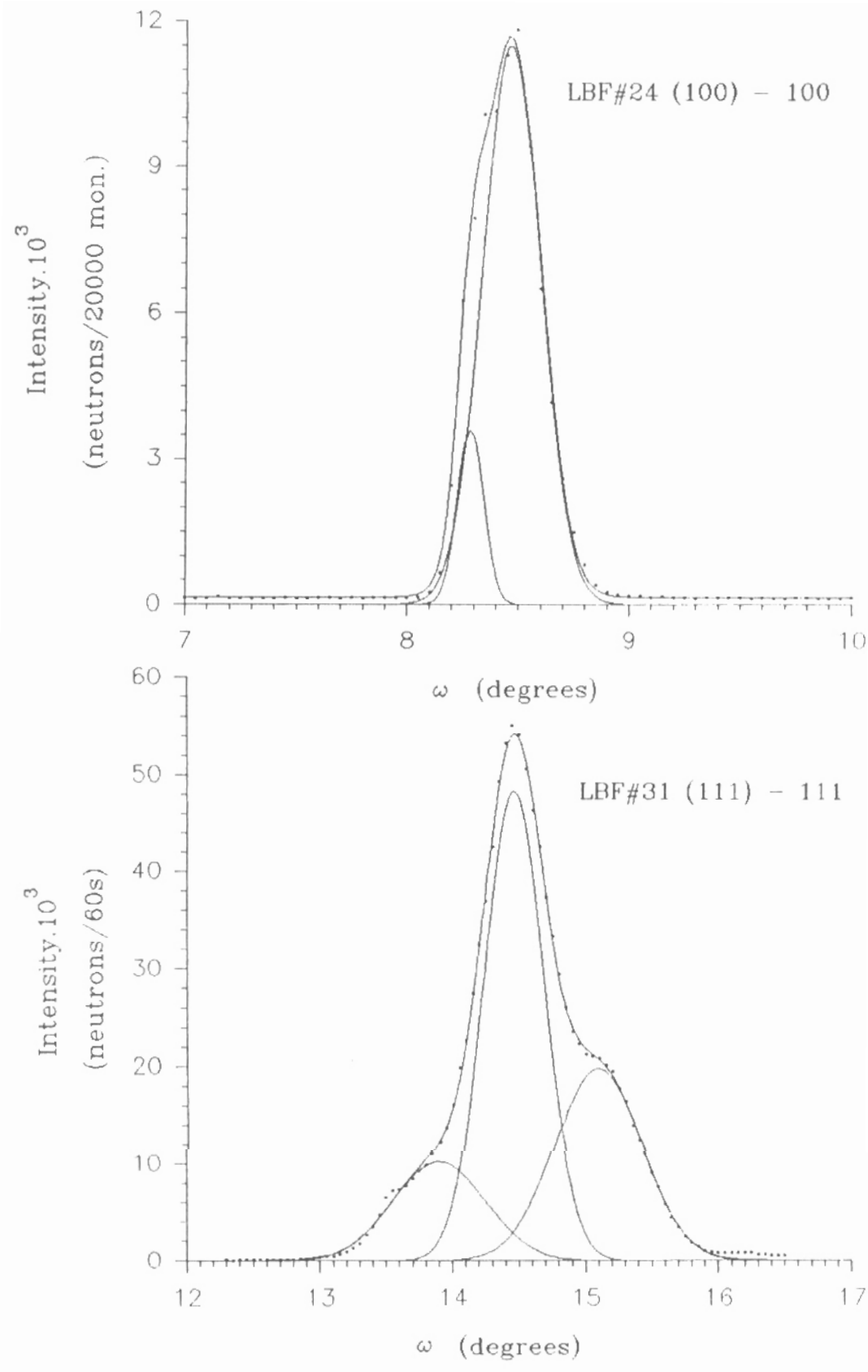

Figure 5 - Rocking curves for the growth direction of samples #24 and #31. Continuous curves correspond to the gaussian fitting for the experimental points.

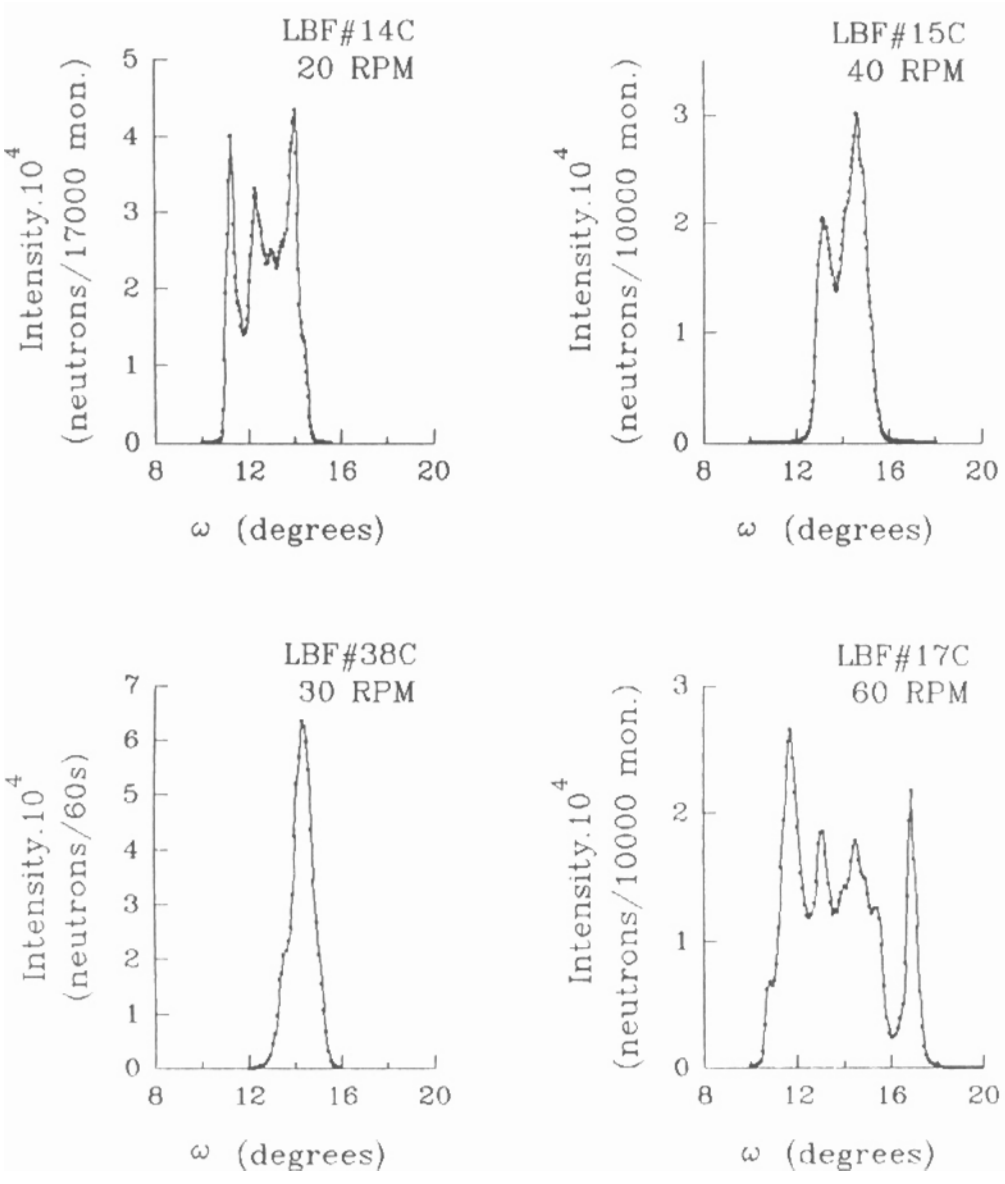

Figure 6 - Rocking curves for the growth direction of samples #14C, #15C, #17C and #38C obtained with different rotation rates.

Research line:

CHARACTERIZATION OF MAGNETIC MATERIALS

Research: **CRYSTALLINE AND MAGNETIC CHARACTERIZATION OF MAGNETITE PRECIPITATES OBTAINED IN THE PREPARATION OF THE Fe_3O_4 + D_2O FERROFLUID.**

K.C. Rodrigues, C.B.R. Parente and V.L. Mazzocchi
Instituto de Pesquisas Energéticas e Nucleares - IPEN-CNEN/SP
A. Roccatto, S. Gama and L.P. Cardoso
Instituto de Física Gleb Wataghin - UNICAMP

Magnetic liquids [1], or ferrofluids, are colloidal suspensions of magnetic particles dispersed in a carrier liquid. Magnetic liquids are stable solutions that react under magnetic fields moving and changing their apparent densities. They have many technological applications such as in optical shutters [2], magnetic seals [3], pressure sensors [4], printers [5]. They also have several medical applications [6,7,8,9,10].

In this work, several different techniques have been used for the crystalline and magnetic characterization of magnetite precipitates obtained in the preparation of the Fe_3O_4 + D_2O ferrofluid. The main objective for the preparation of this ferrofluid is the study, by neutron diffraction, of its behavior under a magnetic field. The small size of the magnetite particles (around 100 A), obtained in the usual preparation method, led to an attempt to increase their sizes. This is necessary to avoid a too large effect of the multiple scattering on the diffracted intensities. To attain this objective, differentiated methods have been employed in the obtention of magnetite precipitates, in the first step of preparation of the Fe_3O_4 + D_2O ferrofluid. The usual preparation method may be divided in two distinct steps. The first step is the obtention of the magnetite precipitate by the action of a base, ammonium hydroxide, on a solution of iron II and III chlorides in water. The second step corresponds to cover the precipitated particles with a dispersing agent (surfactant), in general lauric acid. The differentiated methods involved the application of a magnetic field over the solution where the precipitation occurs, with and without cooling of the solution. The usual preparation method is here called "first method", the method involving application of a magnetic field "second method" and, finally, "third method" for that involving a magnetic field plus cooling of the solution.

Crystalline and magnetic characterization of the precipitated particles, obtained by the three different methods, were done by using neutron diffraction, X-ray diffraction, transmission electron microscopy (TEM) and magnetization measurements. With neutron diffraction, it has been verified a small increase in the signal-to-background ratio for a few reflections from magnetite. This is due to the decrease of the multiple scattering resulting from the enlargement of the mean size of the particles obtained by application of the second and third methods. This can be seen in Fig. 1 where the 111 neutron reflection from three samples of magnetite precipitates, obtained by the application of the three methods, are shown. X-ray diffraction allowed identification of magnetite, Fe_3O_4, as a unique phase in the precipitates. It also allowed determination of the mean size of the particles in the precipitates by means of the Scherrer method (See, for example, the book by Warren [9]). Fig. 2 shows the 311 X-ray reflection from several samples of magnetite precipitates, obtained also by the application of the three methods. By means of photographs obtained by TEM, it was possible to obtain particle size distribution

histograms, mean size, median and standard deviation of the measurements. Fig. 3 shows number frequency histograms, measured with samples of magnetite precipitates obtained in the three methods. The magnetization measurements allowed determination of the magnetic susceptibility and saturation magnetization values for the precipitates, as well as of the ferrofluids with them obtained. The values of magnetization measurements are listed in Table 1.

As main results it can be mentioned those obtained for the precipitates whose preparation methods involved the application of a magnetic field and cooling of the solution. The precipitates, in this case, presented more differentiated values in comparison with those obtained by means of the first method. Increasing of the mean size of the particles has been observed from 120 A to 161 A and from 71.6 A to 103.7 A, for the Scherrer method and electron microscopy, respectively. For the saturation magnetization it was observed an increase from 72.57 emu/g to 77.01 emu/g. These results reflect directly on the characteristics of the ferrofluids, attributing to them better stability and fluidity when under the action of magnetic fields. All main results, obtained in the crystalline and magnetic characterization, are listed in Table 2.

Table 1 - Values for the saturation magnetization (Ms) and magnetic susceptibility (χ) for a few samples of precipitates and ferrofluids.

AMOSTRA	Ms (emu/g)	χ (emu/g.Oe)
MPMT01#02	60,93	$61,99 \times 10^{-2}$
MPMT02#02	71,92	$71,36 \times 10^{-2}$
MPMT03#02	60,72	$69,62 \times 10^{-2}$
FFLMT01	0,1315	$0,04165 \times 10^{-2}$
FFPMT01	0,9724	$0,5996 \times 10^{-2}$
FFLMT02	4,071	$2,7510 \times 10^{-2}$
FFPMT02	1,669	$0,8437 \times 10^{-2}$
FFLMT03	2,352	$1,1660 \times 10^{-2}$
FFPMT03	1,296	$0,5690 \times 10^{-2}$

Table 2 - Results found in the Crystalline and Magnetic Characterization for the Magnetite Precipitates and Ferrofluids.

		CRYSTALLINE CHARACTERIZATION			MAGNETIC CHARACTERIZATION	
METHODS	SAMPLES	NEUTRONS SIG./BG (111)	X-RAYS D (Å)	TEM X (Å)	Ms (emu/g)	χ (emu/g.Oe)
01	MP #01	1.3	126	70	72.57	
	MP #02	1.5	120	71.6	60.93	61.99×10^{-2}
	FF-H_2O				0.1315	0.04165×10^{-2}
	FF-D_2O				0.9724	0.5996×10^{-2}
02	MP #01	1.5	122	110	74.49	
	MP #02	2.0	115	92.0	71.92	71.36×10^{-2}
	FF-H_2O				4.071	2.7510×10^{-2}
	FF-D_2O				1.669	0.8437×10^{-2}
03	MP #01	2.7	161	110	77.01	
	MP #02	1.7	136	103.7	60.72	69.62×10^{-2}
	FF-H_2O				2.352	1.1660×10^{-2}
	FF-D_2O				1.296	0.5690×10^{-2}

REFERENCES

[1] ROSENSWEIG, R.E. Magnetic fluids. Scientific American, 274(4): 136-44, 1982.

[2] MONIN, J.; BREVET-PHILIBERT, O.; NEVEU, S.; DELAUNAY, L.; GAGNAIRE, H. A light polarization modulator using magnetic liquid intended for high precision optical instrumentation. J. Magn. Magn. Mat., 122: 403-05, 1993.

[3] VISLOVICH, A.N.; MEDVEDEV, V.F.; DMITRICHENKO, A.S.; BONDARENKO, G.A.; MOROZOV, V.N.; A magnetic fluid gate as a new element in sealing technology. J. Magn. Magn. Mat., 122: 411-14, 1993.

[4] BACRI, J.C.; LENGLET, J.; PERZYNSKI, R.; SERVAIS, J. Magnetic fluid pressure sensor. J. Magn. Magn. Mat., 122: 399-402, 1993.

[5] MITSUYA, Y.; ABE, T.; MATSUNAGA, S. Novel mechanism of self-injecting magnetic fluid seal applying switch of magnetic force direction on yoke surface. J. Magn. Magn. Mat., 122: 415-19, 1993.

[6] CHAN, D.C.F.; KIRPOTIN, D.B.; BUNN, P.A.Jr. Synthesis and evaluation of colloidal magnetic iron oxides for the site-specific radiofrequency -induced hyperthermia of cancer. J. Magn. Magn. Mat., 122: 374-78, 1993.

[7] MIKHAILIK, O.M.; PANKRATOV, Y.V.; BAKAI, E.A. Biotransformation of intravenously inject finely dispersed iron powders. J. Magn. Magn. Mat., 122: 379-82, 1993.

[8] PAPISOV, M.I.; BOGDANOV Jr., A.; SCHAFFER, B.; NOSSIFF, N.; SHEN, T.; WEISSLEDER, R.; BRADY, T.J. Colloidal magnetic resonance contrast agents: effect of particle surface on biodistribution. J. Magn. Magn. Mat., 122: 383-86, 1993.

[9] RUUGE, E.K.; RUSETSKI, A.N. Magnetic fluids as drug carriers: Targeted transport of drugs by a magnetic field. J. Magn. Magn. Mat., 122: 335-39, 1993.

[10] VLADIMIRSKY, M.A.; KURNETSOV, A.A.; PHILIPPOV, V.I. A magnetic concentration method using hydrosol of ferric particles for diagnosing tuberculois. J. Magn. Magn. Mat., 122: 371-73, 1993.

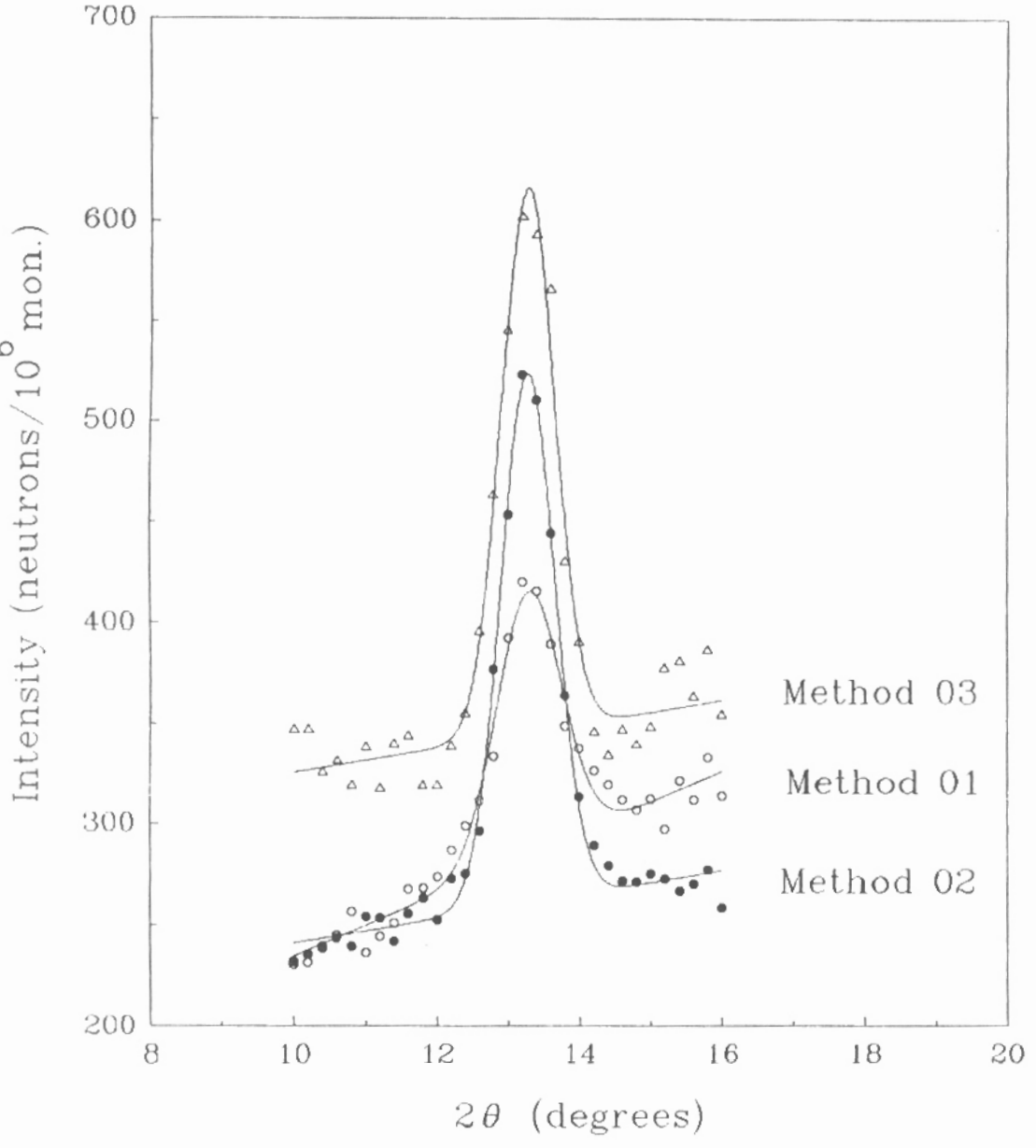

Figure 1 - The 111 neutron reflection from three magnetite precipitate samples obtained in the three different methods. Continuous curves correspond to gaussian fittings to the experimental points.

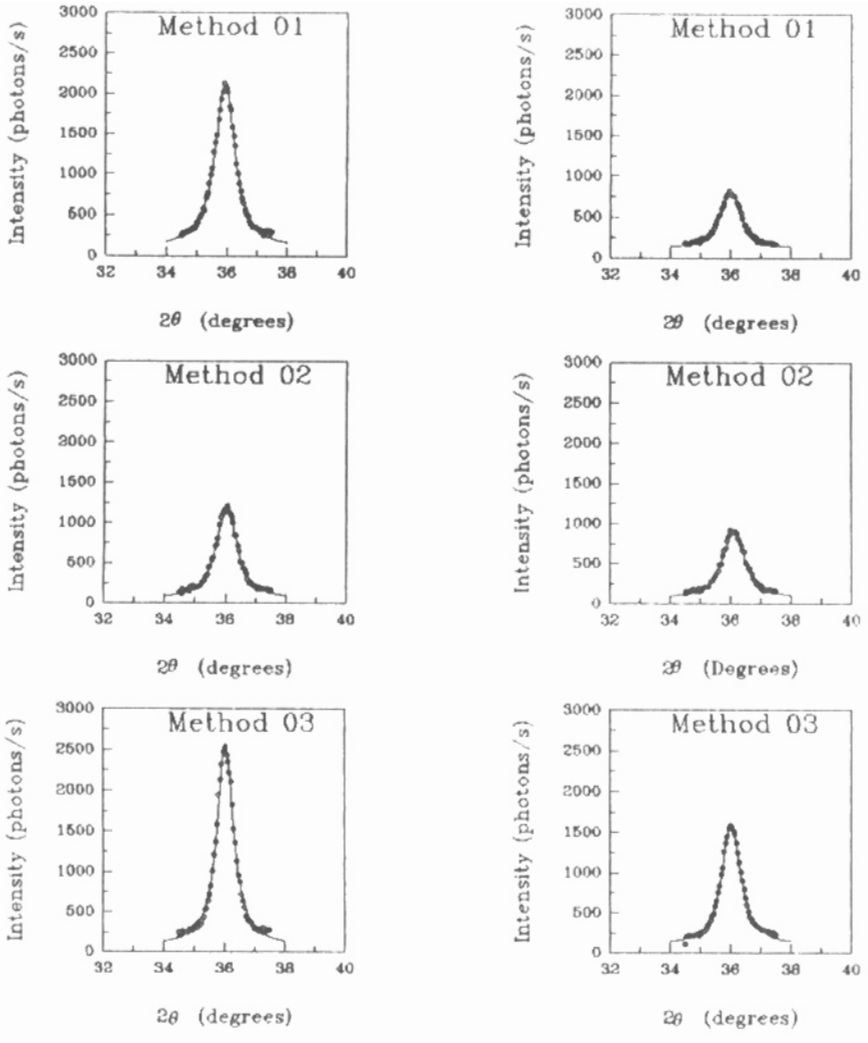

Figure 2 - The 311 X-ray reflection from two series of magnetite precipitate samples obtained in the three different methods. Continuous curves correspond to gaussian fittings to the experimental points.

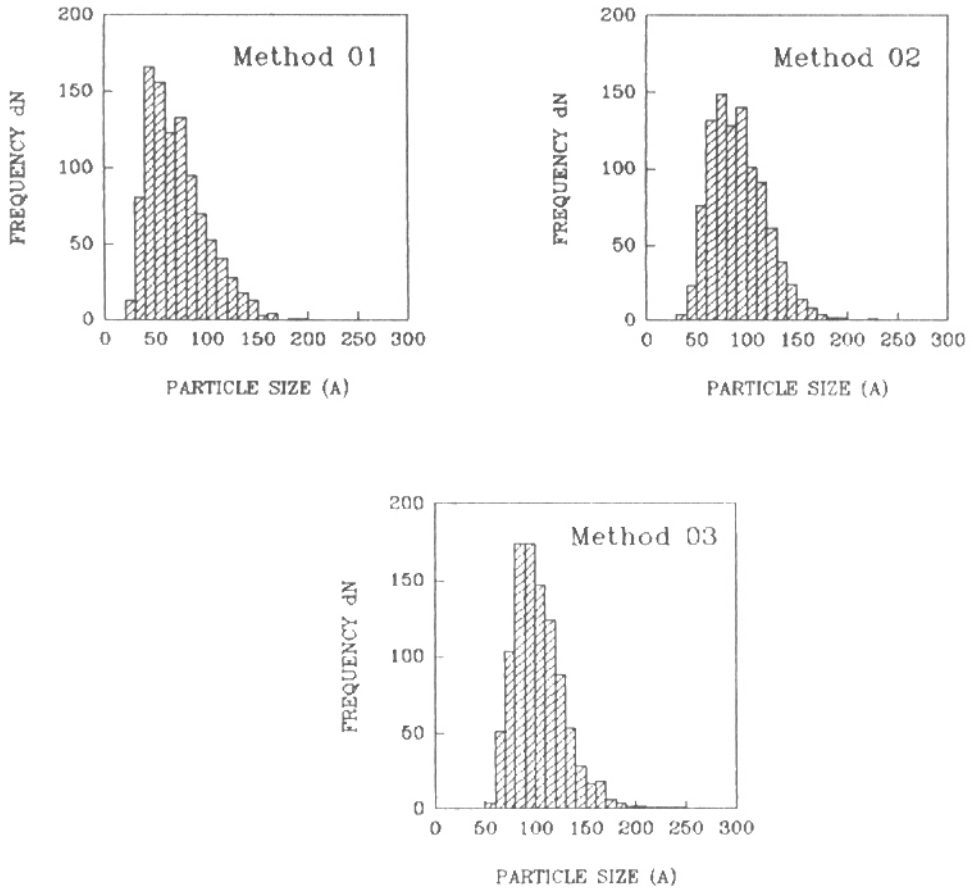

Figure 3 - Number frequency histograms from magnetite precipitate samples obtained in the three different methods.